UPPER BOUND LIMIT ANALYSIS OF SOIL SLOPE STABILITY BASED ON RPIM MESHLESS METHOD

F. T. Liu [1], J. D. Zhao [1], Y. F. Fan [2], and J. H. Yin[3]
[1] Department of Civil and Environmental Engineering,
The Hong Kong University of Science and Technology, Hong Kong, China.
[2] School of Natural Sciences and Humanities,
Harbin Institute of Technology Shen Zhen Graduate School, Shen Zhen, China. Email: yhfan@hit.edu.cn
[3] Department of Civil and Structural Engineering,
The Hong Kong Polytechnic University, Hong Kong, China.

ABSTRACT

Limit analysis is widely used to evaluate the stability of structures in civil engineering. In comparison with elasto-plastic analysis, limit analysis can avoid the complicated computation of incremental analysis. A solution procedure based on radial point interpolation method for upper bound limit analysis of structures is presented. For evaluating the integrations of the external work rate and internal power dissipation rate, a new meshless integration technique based on Cartesian Transformation Method (CTM) was used to transform the domain integral into a boundary integral and a 1D integral. Finally, the nonlinear optimization problem derived from the upper bound limit analysis can be solved based on distinguishing rigid/plastic zones. And some examples of stability analysis show that this approach is a valid and simple technique.

KEYWORDS

Slope stability; Upper bound limit analysis; Radial point interpolation method; nonlinear programming; Cartesian Transformation Method (CTM)

INTRODUCTION

Limit analysis is a powerful method for stability analysis and limit bearing capacity of engineering structures. In geotechnical engineering, upper bound limit analysis is widely used to analyze the slope stability. Drucker (1952) firstly presented limit analysis based on plastic limit theorem, and then Chen (1975) introduced limit analysis into the geotechnical engineering for analyzing the bearing capacity, earth pressure on retaining wall and slope stability. It takes advantage of the lower and upper theorems of classical plasticity to bracket the true solution from a lower bound to an upper bound. However, it is difficult to obtain analytical solution for practical engineering, and numerical approaches are often required for limit analysis. In the past three decades, many studies have been devoted to developing numerical methods of limit analysis.

Many researchers (Lysmer 1970; Anderheggen and Knopfel 1972; Bottero et al. 1980; Sloan 1988, 1989; Sloan and Kleeman 1995) constructed numerical limit analysis based on finite element method and linear programming theory, where the general yield criterion often was linearized to a convex polyhedron, and the nonlinear inequalities were approximated by a set of linear inequalities. Especially for the slope stability analysis, following the related work by Sloan and Kleeman (1995), some researchers (Yu et al. 1998; Kim et al. 1999; Kim et al. 2002, etc) have applied the lower and upper bound approach to evaluate the slope stability. On the other hand, following the work of Zouain et al. (1993), Lyamin and Sloan (2002) proposed a nonlinear numerical method to perform upper and lower bound limit analysis based on linear finite elements and nonlinear programming. The results showed that their approach is vastly superior to a widely used linear programming formulation, especially for large scale applications. However, this approach has a potential difficulty in applying these formulations is that special stress or displacement finite elements need to be used. Therefore, an alternative nonlinear technique which named the direct iterative algorithm is used to perform limit analysis of non-frictional materials (Zhang et al., 1991; Liu et al., 1995; Capsoni and Corradi, 1997). Following these ideas, Li and Yu (2006) extended the direct iterative algorithm to calculate plastic collapse loads of 2D and 3D structures obeying the ellipsoid yield criterion. In these approaches, upper bound limit analysis of structures is formulated as a nonlinear optimization problem with a single equality constraint, and a technique based on distinguishing rigid/plastic zones was adopted to solve this special nonlinear constrained optimization problem.

Recently, as the development of finite element method, a so-called 'meshless' method has attracted more attention in the field of numerical method. Recently, Chen et al. (2008) and Le et al. (2009, 2010) constructed lower and upper formulation of limit analysis based element-free Galerkin (EFG) method which first proposed by Belytschko et al. (1994). Although the EFG method has been successfully applied to the lower and upper bound approaches, two issues are still not well studied: 1) difficulties in the enforcement of essential boundary conditions. This is because its shape function which calculated based on the moving least square method (MLS) is lack of Kronecher delta function property, i.e., where is the Kronecker delta function; 2) complexity in numerical algorithms for calculating shape function and its derivatives. For two issues, the one of approach is so-called radial point interpolation method (RPIM) proposed by Wang and Liu (2002). The RPIM shape functions have the Kronecker delta function property and partitions of unity. Therefore, the essential boundary conditions could be easily enforced. Furthermore, the accuracy of RPIM is higher than that of the MLS (Liu and Gu 2005). On the other hand, regarding the integral strategy, some truly meshless methods commonly rely on the nodal integration technique. However, direct nodal integration is unstable because of under-integration and vanishing derivatives of shape functions at the nodes. To overcome this difficulty, Beissel and Belytschko (1996) added a residual of the equilibrium equation terms to the potential energy functional for stabilizing nodal integration. However, Beissel and Belytschko (1996) stated that the accuracy of this method is less than that of the original EFG method. Up-to-date stabilized conforming nodal integration technique is proposed by Chen et al. (2001, 2002), they modified the shape functions prior to nodal integration, even though this method is considered as a robust integration technique, it is based on the construction of a Voronoi diagram. So it cannot be considered a true meshless method. Recently, Khosravifard and Hematiyan (2010) proposed a new meshless integration technique based on Cartesian Transformation Method (CTM), in their method a domain integral is transformed into a boundary integral and a 1D integral.

In this paper, we reformulated the upper bound limit analysis of structures using the nonlinear programming theory and the RPIM method, and the new integration technique proposed by Khosravifard and Hematiyan (2010) to calculate the internal dissipation power and external work rate. And the present method was used to calculate the limit loading parameter of a vertical slope. The layout of this paper is as follows: Section 2 briefly describes the upper bound limit analysis formulation for an ellipsoid yield function using RPIM method and CTM integration. A direct iterative algorithm based on Lagrange method is used to solve the nonlinear programming problem in Section 3. Numerical example for vertical slope is provided in Section 4 to illustrate the validity of the present method.

NUMERICAL FORMULATION FOR UPPER BOUND APPROACH BASED ON RPIM MESHLESS METHOD

The upper bound theorem

The upper bound theorem of limit analysis states: among all kinematically admissible velocities (that is the plastic admissible strains), the real one yields the lowest rate of plastic dissipation power (Drucker and Prager 1952)

$$\int_V D\left(\dot{\boldsymbol{\varepsilon}}^*\right) dV \geq \int_{\Gamma_\sigma} \mathbf{T}^T \mathbf{u}^* d\Gamma + \lambda \int_V \mathbf{f}^T \mathbf{u}^* dV \tag{1}$$

where λ is the limit load multiplier, $\mathbf{T}$ is the basic load vector of surface tractions, $\mathbf{f}$ is the body force vector, $\mathbf{u}^*$ is the kinematic admissible velocity vector, $D(\dot{\boldsymbol{\varepsilon}}^*)$ denotes the function for the rate of the plastic dissipation power in terms of the admissible strain rate $\dot{\boldsymbol{\varepsilon}}^*$, Γ_σ denotes the traction boundary, and V denotes the space domain of the structure. Here, the kinematic admissible velocity vector $\mathbf{u}^*$ must satisfy the following two conditions (Chen 2002):

1) Compatibility and velocity bound conditions

$$\dot{\boldsymbol{\varepsilon}}^* = \frac{1}{2}\left(\nabla \mathbf{u}^* + \mathbf{u}^* \nabla\right) \quad \text{in } V \tag{2a}$$

$$\mathbf{u}^* = \overline{\mathbf{u}} \quad \text{on } \Gamma_u \tag{2b}$$

2) The yield criteria function

$$f(\boldsymbol{\sigma}) = 0 \tag{3}$$

The above two conditions can be related by the associated flow rule, i.e.,

$$\dot{\boldsymbol{\varepsilon}}^* = \mu \frac{\partial f}{\partial \boldsymbol{\sigma}} \tag{4}$$

where Γ_u denotes the displacement boundary; μ is the non-negative plastic multiplier. Therefore, the solution of limit load multiplier based on upper bound theorem can be formulated as the following mathematical programming problems (the surface traction is omitted)

$$\begin{aligned} &\lambda = \min \int_V D\left(\dot{\boldsymbol{\varepsilon}}^*\right) dV \\ &s.t. \quad \int_V \mathbf{f}^T \mathbf{u}^* dV = 1 \\ &\qquad \dot{\boldsymbol{\varepsilon}}^* = \frac{1}{2}\left(\nabla \mathbf{u}^* + \mathbf{u}^* \nabla\right) \quad \text{in } V \\ &\qquad \mathbf{u}^* = \bar{\mathbf{u}} \qquad\qquad \text{on } \Gamma_u \end{aligned} \tag{5}$$

From the optimum of limit loading multiplier λ_{opt}, the limit loading can be computed according to the following equation:

$$\mathbf{f}_{\text{lim}} = \lambda_{\text{opt}} \cdot \mathbf{f} \tag{6}$$

Nonlinear optimization problems for the plane strain von-Mises yield criterion

In general, the slope stability problems are treated as the plain strain problems in geotechnical engineering. For the plain strain condition, the von-Mises (or Tresca) yield criterion can be written as (Pastor, 2000)

$$f\left(\boldsymbol{\sigma}\right) = \sqrt{\frac{1}{4}\left(\sigma_x - \sigma_y\right)^2 + \tau_{xy}^2} - c = 0 \tag{7}$$

where c is the cohesion. According to the associated flow rule, the power of dissipation can be formulated as a function of strain rates as (Capsoni and Corradi, 1997)

$$D\left(\dot{\boldsymbol{\varepsilon}}\right) = \sqrt{\dot{\boldsymbol{\varepsilon}}^T \boldsymbol{\Theta} \dot{\boldsymbol{\varepsilon}}} \tag{8}$$

where

$$\boldsymbol{\Theta} = \begin{bmatrix} c^2 & -c^2 & 0 \\ -c^2 & c^2 & 0 \\ 0 & 0 & c^2 \end{bmatrix} \tag{9}$$

Therefore, the mathematical programming problem (5) of finding the upper bound solution of limit loading multiplier can be formulated as the following nonlinear optimization problem:

$$\begin{aligned} &\lambda = \min \int_V \sqrt{\dot{\boldsymbol{\varepsilon}}^T \boldsymbol{\Theta} \dot{\boldsymbol{\varepsilon}}}\, dV \\ &s.t. \quad \int_V \mathbf{f}^T \mathbf{u}^* dV = 1 \\ &\qquad \dot{\boldsymbol{\varepsilon}}^* = \frac{1}{2}\left(\nabla \mathbf{u}^* + \mathbf{u}^* \nabla\right) \quad \text{in } V \\ &\qquad \mathbf{u}^* = \bar{\mathbf{u}} \qquad\qquad \text{on } \Gamma_u \end{aligned} \tag{10}$$

Radial point interpolation method

The approximation of the field variables of interest $\mathbf{x}$ using radial point interpolation method (RPIM) can be expressed in the following form (Liu and Gu, 2005):

$$u(\mathbf{x}) = \left[\mathbf{R}_q^T\left(\mathbf{x}\right) \quad \mathbf{P}_m^T\left(\mathbf{x}\right)\right] \mathbf{G}^{-1} \begin{Bmatrix} \mathbf{U}_s \\ \mathbf{0} \end{Bmatrix} = \boldsymbol{\Phi}\left(\mathbf{x}\right) \mathbf{U}_s \tag{7}$$

where $u(\mathbf{x})$ is the function of field variables, $\mathbf{U}_s=\{u_1, u_2, \ldots, u_n\}^T$ is the vector of function values, $\boldsymbol{\Phi}(\mathbf{x})$ is the RPIM shape functions corresponding to the nodal value and given by

$$\boldsymbol{\Phi}\left(\mathbf{x}\right) = \left[\mathbf{R}_q^T\left(\mathbf{x}\right) \quad \mathbf{P}_m^T\left(\mathbf{x}\right)\right] \mathbf{G}^{-1} = \left[\phi_1\left(\mathbf{x}\right) \quad \phi_2\left(\mathbf{x}\right) \quad \cdots \quad \phi_n\left(\mathbf{x}\right)\right] \tag{8}$$

in which, $\mathbf{R}_q$ is the moment matrix of the radial basis function (RBF) given by

$$\mathbf{R}_q = \begin{bmatrix} R_1\left(\mathbf{x}_1\right) & R_2\left(\mathbf{x}_1\right) & \cdots & R_n\left(\mathbf{x}_1\right) \\ R_1\left(\mathbf{x}_2\right) & R_2\left(\mathbf{x}_2\right) & \cdots & R_n\left(\mathbf{x}_2\right) \\ \vdots & \vdots & \ddots & \vdots \\ R_1\left(\mathbf{x}_n\right) & R_2\left(\mathbf{x}_n\right) & \cdots & R_n\left(\mathbf{x}_n\right) \end{bmatrix}_{n\times n} \tag{9}$$

and $\mathbf{P}_m$ the polynomial moment matrix is defined as follows

$$\mathbf{P}_m=\begin{bmatrix} p_1(\mathbf{x}_1) & p_2(\mathbf{x}_1) & \cdots & p_m(\mathbf{x}_1) \\ p_1(\mathbf{x}_2) & p_2(\mathbf{x}_2) & \cdots & p_m(\mathbf{x}_2) \\ \vdots & \vdots & \ddots & \vdots \\ p_1(\mathbf{x}_n) & p_2(\mathbf{x}_n) & \cdots & p_m(\mathbf{x}_n) \end{bmatrix}_{n\times m} \tag{10}$$

and the matrix **G** is defined as

$$\mathbf{G}=\begin{bmatrix} \mathbf{R}_q & \mathbf{P}_m \\ \mathbf{P}_m^T & \mathbf{0} \end{bmatrix} \tag{11}$$

Therefore, the k-th element of shape function can be expressed as follows,

$$\phi_k(\mathbf{x})=\sum_{i=1}^{n}R_i(\mathbf{x})G_{(i,k)}+\sum_{j=1}^{m}p_j(\mathbf{x})G_{(n+j,k)} \tag{12}$$

where $G_{(i,k)}$ is the element of matrix $\mathbf{G}^{-1}$. A classical RBF is multiquadric basis (MQ), which has the following form (Gu and Liu, 2005):

$$R_i(\mathbf{x})=\left[(x-x_i)^2+(y-y_i)^2+(\alpha_c d_c)^2\right]^q \tag{13}$$

where α_c and q are two shape parameters, d_c is the character length that relates to the nodal spacing in the local support domain. In addition, the complete polynomial basis of order p for two-dimensional domains can be written in the following form (Gu and Liu, 2005):

$$\mathbf{P}^T(\mathbf{x})=\{1 \quad x \quad y \quad x^2 \quad xy \quad y^2 \quad \cdots \quad x^p \quad y^p\} \tag{14}$$

If the function $\mathbf{u}(\mathbf{x})$ stands for the displacement field for two-dimensional domains, it can be interpolated from the vectors of nodal function value and RPIM shape function corresponding to the nodal value, i.e.,

$$\mathbf{u}(\mathbf{x})=\sum_{I=1}^{n}\begin{bmatrix} \phi_I & 0 \\ 0 & \phi_I \end{bmatrix}\begin{bmatrix} u_I \\ v_I \end{bmatrix}=\sum_{I=1}^{n}\mathbf{\Phi}_I(\mathbf{x})\mathbf{u}_I \tag{15}$$

where $\mathbf{\Phi}_I(\mathbf{x})$ is the matrix of shape function of node I, and $\mathbf{u}_I$ is the nodal displacements. And, the derivatives of the RPIM shape functions can be formulated as follows (Wang and Liu 2002):

$$\frac{\partial\phi_k}{\partial x}=\sum_{i=1}^{n}\frac{\partial R_i}{\partial x}G_{(i,k)}+\sum_{j=1}^{m}\frac{\partial p_j}{\partial x}G_{(n+j,k)} \tag{17a}$$

$$\frac{\partial\phi_k}{\partial y}=\sum_{i=1}^{n}\frac{\partial R_i}{\partial y}G_{(i,k)}+\sum_{j=1}^{m}\frac{\partial p_j}{\partial y}G_{(n+j,k)} \tag{17b}$$

According to the approximation of displacement field function, the plastic admissible strains can be expressed as

$$\boldsymbol{\varepsilon}=\mathbf{L}\mathbf{u}(\mathbf{x})=\begin{bmatrix} \frac{\partial}{\partial x} & 0 \\ 0 & \frac{\partial}{\partial y} \\ \frac{\partial}{\partial y} & \frac{\partial}{\partial x} \end{bmatrix}\begin{bmatrix} \phi_1(\mathbf{x}) & 0 & \cdots & \phi_n(\mathbf{x}) & 0 \\ 0 & \phi_1(\mathbf{x}) & \cdots & 0 & \phi_n(\mathbf{x}) \end{bmatrix}\begin{bmatrix} u_1 \\ v_1 \\ \vdots \\ u_n \\ v_n \end{bmatrix}=\begin{bmatrix} \frac{\partial\phi_1}{\partial x} & 0 & \cdots & \frac{\partial\phi_n}{\partial x} & 0 \\ 0 & \frac{\partial\phi_1}{\partial y} & \cdots & 0 & \frac{\partial\phi_n}{\partial y} \\ \frac{\partial\phi_1}{\partial y} & \frac{\partial\phi_1}{\partial x} & \cdots & \frac{\partial\phi_n}{\partial y} & \frac{\partial\phi_n}{\partial x} \end{bmatrix}\begin{bmatrix} u_1 \\ v_1 \\ \vdots \\ u_n \\ v_n \end{bmatrix}=\mathbf{B}\mathbf{u} \tag{18}$$

where **B** is the strain matrix. Therefore, substituting Eq. (18) into nonlinear programming problem, the discretized formulation of upper bound approach based on RPIM meshless method can be expressed as follows:

$$\begin{aligned} &\lambda=\min \int_V \sqrt{\mathbf{u}_I^T\mathbf{B}^T\mathbf{\Theta}\mathbf{B}\mathbf{u}_I}\,dV \\ &s.t. \quad \int_V \mathbf{f}^T\mathbf{\Phi}\mathbf{u}_I\,dV=1 \\ &\quad \mathbf{u}=\bar{\mathbf{u}} \qquad \text{on } \Gamma_u \end{aligned} \tag{19}$$

A new integration method based on CTM

In the numerical formulation of nonlinear programming problem (19) based on RPIM, the main task is to calculate the integration in the objective function and constrained equations. Recently, Khosravifard and Hematiyan (2010) proposed a new meshless integration technique based on Cartesian Transformation Method

(CTM), in their method a domain integral is transformed into a boundary integral and a 1D integral. According to the CTM integral technique, the integral can be calculated in terms of the following formulation, for 2D problems:

$$I = \mathbf{W}^{2D} \cdot \mathbf{F} = \sum_{i=1}^{n_G} W^{2D}(\mathbf{x}_i) f(\mathbf{x}_i) \tag{20}$$

where

$$W^{2D}(\mathbf{x}_i) = J_i^x \cdot J_i^y \cdot w_i^x \cdot w_i^y$$

and $\mathbf{x}_i$ is the Gaussian points, i=1,…,n_G, where n_G is the number of the Gaussian points. Furthermore, by introducing the transformation matrix $\mathbf{C}_e$, the nodal velocity vector $\mathbf{u}_I$ for each node can be expressed by the global nodal velocity vector $\mathbf{U}$ for the slope, i.e

$$\mathbf{u}_I = \mathbf{C}_e \mathbf{U} \tag{21}$$

Therefore, the objective function of nonlinear programming problem (19) can be reformulated as follows:

$$I = \sum_{i=1}^{n_G} W^{2D}(\mathbf{x}_i) \sqrt{\mathbf{U}^T \mathbf{K}_i \mathbf{U}} \tag{22}$$

where

$$\mathbf{K}_i = \mathbf{C}_e^T \mathbf{D}^T \mathbf{\Theta} \mathbf{D} \mathbf{C}_e$$

On the other hand, the integral of external work rate can be calculated by using 1-D Gaussian quadrature method, and the nodal traction force vector $\mathbf{F}$ can be expressed as follows

$$\mathbf{F}^T = \sum_{l}^{n_{ct}} \sum_{i=1}^{n_{Gt}} J_{il} w(\mathbf{x}_i) \mathbf{f}(\mathbf{x}_i)^T \mathbf{\Phi} \cdot \mathbf{C}_e \tag{23}$$

Therefore, the RPIM formulation of nonlinear programming (19) can be finally expressed as follows:

$$\begin{aligned} &\lambda = \min \sum_{i=1}^{n_G} W^{2D}(\mathbf{x}_i) \cdot \sqrt{\mathbf{U}^T \mathbf{K}_i \mathbf{U}} \\ &s.t. \quad \mathbf{F}^T \cdot \mathbf{U} = 1 \\ &\qquad \mathbf{K}_v \mathbf{U} = 0 \\ &\qquad \mathbf{u} = 0 \qquad \text{on } \Gamma_u \end{aligned} \tag{24}$$

where $\mathbf{K}_v\mathbf{U}$=0 is the plastic incompressibility should be satisfied for the materials with von Mises' or Hill's yield criterion, the matrix $\mathbf{K}_v$ can be expressed as follows:

$$\mathbf{K}_v = \mathbf{D}_v \mathbf{C}_e; \quad \mathbf{D}_v = \begin{bmatrix} \mathbf{D}_{v1} & \mathbf{D}_{v2} & \cdots & \mathbf{D}_{vn} \end{bmatrix}; \quad \mathbf{D}_{vi} = \begin{bmatrix} \phi_{i,x} & \phi_{i,y} \end{bmatrix}; \quad i = 1, \cdots, n$$

In addition, it should be pointed out the velocity boundary conditions can be imposed by means of the conventional finite element technique due to the use of radial point interpolation shape function in this study.

THE DIRECT ITERATIVE METHOD

For the nonlinear programming problem (24), there is a calculation of square root which could make the objective function unsmooth and nondifferentiable. This causes some difficulties in solving the nonlinear programming problem. Following the work of Li and Yu (2006), it can be overcome using an iterative algorithm for distinguishing rigid/plastic zones. At first, the NLP (24) are transformed into an unconstrained optimization problem using Lagrange method. The Lagrange function is the following form:

$$L(\mathbf{U}, \mu) = \sum_{i=1}^{n_G} W^{2D}(\mathbf{x}_i) \cdot \sqrt{\mathbf{U}^T \mathbf{K}_i \mathbf{U}} + \alpha \sum_{i=1}^{n_G} W^{2D}(\mathbf{x}_i) \cdot (\mathbf{K}_v \mathbf{U})^T \mathbf{K}_v \mathbf{U} + 2\mu(1 - \mathbf{F}^T \cdot \mathbf{U}) \tag{25}$$

where μ is the Lagrange multiplier. Following the work of Li and Yu (2005), an iterative control parameter ω^{ICP} was defined as follows:

$$\omega^{ICP} = \sqrt{\mathbf{U}^T \mathbf{K}_i \mathbf{U}} \tag{26}$$

And then, the Lagrange function can be reformulated as:

$$L(\mathbf{U}, \mu) = \sum_{i=1}^{n_G} W^{2D}(\mathbf{x}_i) \cdot \frac{(\mathbf{U}^T \mathbf{K}_i \mathbf{U})}{\omega^{ICP}} + \alpha \sum_{i=1}^{n_G} W^{2D}(\mathbf{x}_i) \cdot (\mathbf{K}_v \mathbf{U})^T \mathbf{K}_v \mathbf{U} + 2\mu(1 - \mathbf{F}^T \cdot \mathbf{U}) \tag{27}$$

For finding all rigid regions, the following iterative process is needed.

Step1: initializing the nonlinear objective function

Let iterative control parameter ω^{ICP}=1, then, the initial nodal displacement velocity can be estimated by solving the following equation system:

$$\begin{cases} \sum_{i=1}^{n_G} W^{2D}\left(\mathbf{x}_i\right)\cdot\left(\mathbf{K}_i+\alpha\mathbf{K}_v^T\mathbf{K}_v\right)\mathbf{U}_0=\mu_0\mathbf{F} \\ \mathbf{f}^T\mathbf{U}_0=1 \end{cases} \tag{28}$$

and the initial load multiplier can be calculated by using:

$$\lambda_0=\sum_{i=1}^{n_G} W^{2D}\left(\mathbf{x}_i\right)\cdot\sqrt{\mathbf{U}_0^T\mathbf{K}_i\mathbf{U}_0} \tag{29}$$

Step k+1 (k=0, 1, 2 …): distinguishing the nondifferentiable areas to revise the objective function

Based on the results at step k, the value of ω^{ICP} need to be calculated at very Gaussian integral point of CTM, then the Gaussian integral point set S will be subdivided into two subsets: the subset S_r^{k+1} where the object function is not differentiable and the subset S_P^{k+1} where the object function is differentiable, i.e.,

$$S_r^{k+1}=\left\{i\in S,\omega^{ICP}=0\right\};\quad S_p^{k+1}=\left\{i\in S,\omega^{ICP}\neq 0\right\} \tag{30}$$

For ω^{ICP}=0, the original optimization problem can be solved in terms of the following problem:

$$\begin{aligned} &\min_{\mathbf{U}} \sum_{i\in S_p^{k+1}}^{n_G} W^{2D}\left(\mathbf{x}_i\right)\cdot\frac{\mathbf{U}_{k+1}^T\mathbf{K}_i\mathbf{U}_{k+1}}{\sqrt{\mathbf{U}_k^T\mathbf{K}_i\mathbf{U}_k}} \\ &s.t.\ \mathbf{f}^T\mathbf{U}_{k+1}=1 \\ &\quad\left(\mathbf{K}_v\mathbf{U}_{k+1}\right)_i=0 \quad \left(i\in S\right) \\ &\quad\mathbf{U}_{k+1}^T\mathbf{K}_i\mathbf{U}_{k+1}=0 \quad \left(i\in S_r^{k+1}\right) \end{aligned} \tag{31}$$

The revised NLP problem can be solved in terms of the following equation system:

$$\begin{cases} \sum_{i\in S_p^{k+1}} W^{2D}\left(\mathbf{x}_i\right)\cdot\frac{\mathbf{K}_i\mathbf{U}_{k+1}}{\sqrt{\mathbf{U}_k^T\mathbf{K}_i\mathbf{U}_k}}+\xi\sum_{i\in S_r^{k+1}} W^{2D}\left(\mathbf{x}_i\right)\cdot\mathbf{K}_i\mathbf{U}_{k+1}+\alpha\sum_{i\in S_r^{k+1}} W^{2D}\left(\mathbf{x}_i\right)\cdot\mathbf{K}_v^T\mathbf{K}_v\mathbf{U}_{k+1}=\mu_{k+1}\mathbf{F} \\ \mathbf{F}^T\mathbf{U}_{k+1}=1 \end{cases} \tag{32}$$

By solving the Eq. (32), we can obtain the nodal velocity and limit load multiplier at this step

$$\lambda_{k+1}=\sum_{i=1}^{n_G} W^{2D}\left(\mathbf{x}_i\right)\cdot\sqrt{\mathbf{U}_{k+1}^T\mathbf{K}_i\mathbf{U}_{k+1}} \tag{33}$$

The above iterative process is repeated until the following convergence criteria are satisfied

$$\frac{\left|\lambda_{k+1}-\lambda_k\right|}{\lambda_{k+1}}\leq\eta_1;\quad \frac{\left\|\mathbf{U}_{k+1}-\mathbf{U}_k\right\|}{\mathbf{U}_{k+1}}\leq\eta_2 \tag{34}$$

where η_1 and η_2 are the computational error tolerances.

UPPER BOUND FOR THE HEIGHT LIMIT OF A VERTICAL SLOPE

The height limit of a vertical slope is a classical problem of limit analysis or yield design theory. The vertical slope (See Figure 1) is subjected only to own weight. The soil is homogeneous and isotropic, and its cohesion is c, unit weight is γ. According to the research by Pastor et al. (2000), the new bounds of limit loading parameter is as follows:

$$3.7603\leq Q_\gamma=\frac{\gamma H}{c}\leq 3.7859 \tag{35}$$

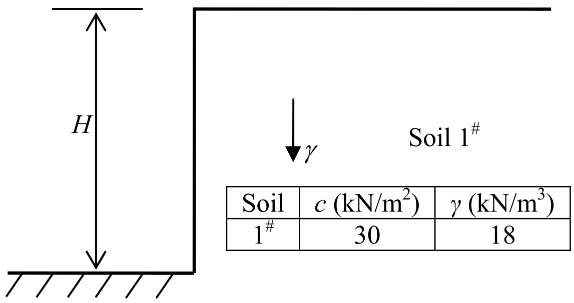

Figure 1 The model of critical height of a vertical slope

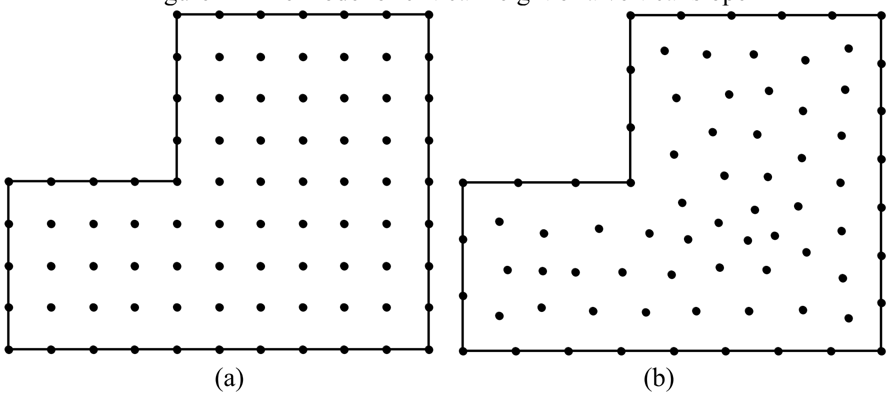

Figure 2 The layout of the field nodes: (a) regular; (b) irregular

For this test problem, two types of layout of field nodes as shown in Figure 2 can be used to discretize the domain. And then, the RPIM shape function can be constructed based on the discretization of field nodes. For a reliable RPIM shape function construction, a T2L-Scheme proposed by Liu (2010) is used to select local supporting nodes. On the other hand, the interpolation accuracy of RPIM can also be affected by the dimensionless shape parameters α_c, q and numbers of field nodes. Therefore, these parameters should be analysed one by one.

Firstly, the shape parameters α_c=4 and q=0.5 are fixed for analysing the effect of nodal layout on the limit loading parameter Q_γ. In addition, the optimal parameters for the direct iterative algorithm can be chose according to the research of Li and Yu (2006). And the computational error tolerances η_1=η_2=0.001 are fixed.

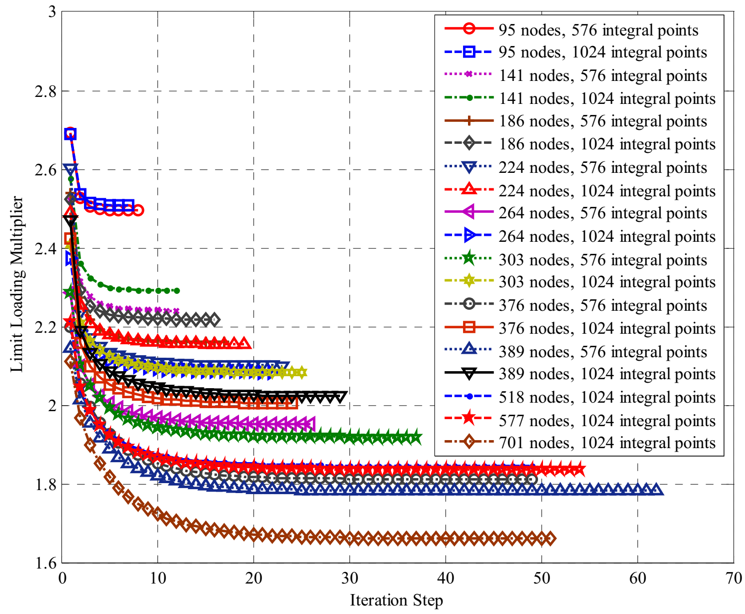

Figure 3 The convergence sequence of limit loading multiplier with iterative steps for irregular nodal layout

Table 1 The results of limit load multiplier for irregular nodal layout (576 integral points)

Nodes	95	141	186	224	264	303	376	389
λ	2.496	2.242	2.163	2.102	1.954	1.921	1.814	1.784
Q_γ	9.985	8.968	8.650	8.407	7.825	7.682	7.257	7.137
errors	58%	42%	37%	33%	23%	21%	15%	13%
Runtime (s)	--	--	--	29	48	92	195	171

Table 2 The results of limit load multiplier for irregular nodal layout (1024 integral points)

Nodes	95	141	186	224	264	303	376	389	518	577	701
λ	2.509	2.293	2.219	2.157	2.086	2.084	2.007	2.025	1.847	1.837	1.662
Q_γ	10.037	9.170	8.877	8.627	8.345	8.335	8.028	8.098	7.387	7.348	6.650
errors	59%	45%	41%	37%	32%	32%	27%	28%	17%	16%	0.5%
Runtime (s)	--	--	--	42	73	112	171	171	701	902	1360

With the above parameters, the optimal value of limit loading multiplier can be found using the direct iterative algorithm based on regular and irregular nodal layout. The convergence of limit loading multiplier with iterative steps for irregular nodal layout is shown in Figure 3. The optimal value of limit multiplier and the corresponding limit loading parameter for 576 and 1024 integral points are shown in Table 1 and Table2 respectively. As the same numbers of integral point, the accuracy of limit loading parameter will increase with the increasing numbers of field node (see Figure 5a). For regular nodal layout, the convergence sequence of limit multiplier with iterative steps is shown in Figure 4. And the optimal value of limit multiplier and the corresponding limit loading parameter for different integral points are shown in Table 3. In this case, the number of integral points dependents on that of field nodes, hence, the accuracy of limit loading parameter is analysed just for the different numbers of field node. From the Figure 5b and Table3, the accuracy of limit loading parameter will also increase with the increasing numbers of field node.

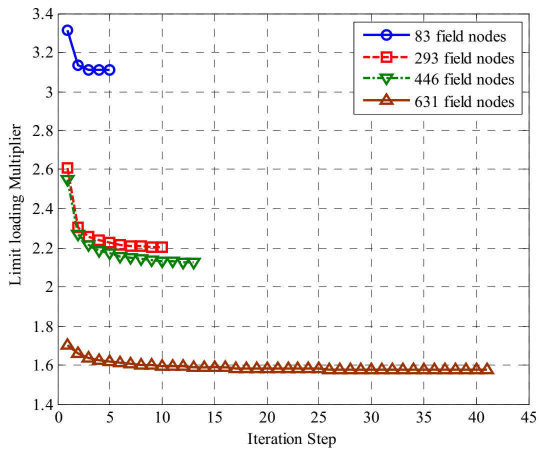

Figure 4 The convergence sequence of limit loading multiplier with iterative steps for regular nodal layout

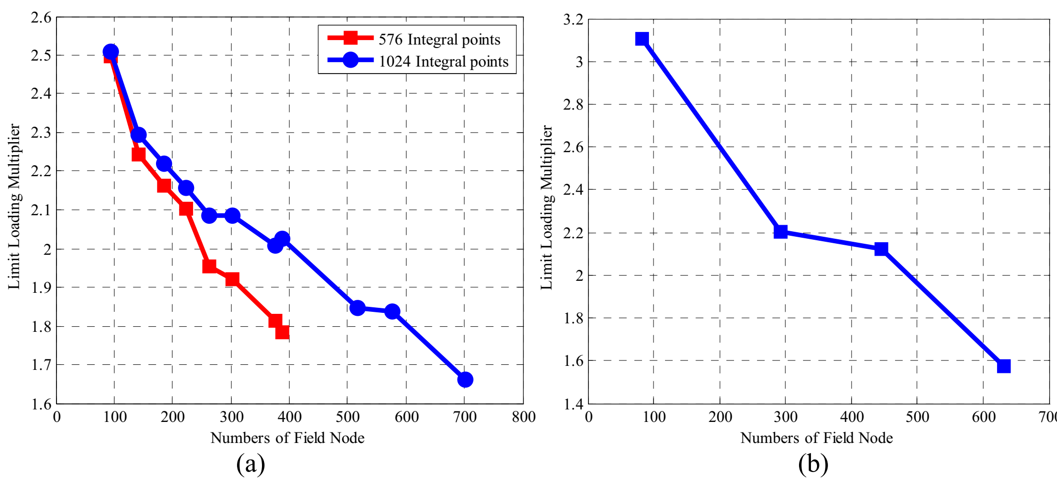

Figure 5 The limit loading multiplier with different numbers of field nodes: (a) irregular nodal layout, and (b) regular nodal layout

Table 3 The results of limit load multiplier for irregular nodal layout

Nodes	83	293	446	631
λ	3.108	2.203	2.215	1.575
Q_γ	12.432	8.813	8.500	6.287
errors	97%	40%	35%	0.04%
Runtime (s)	0.1	35	194	1169

By comparing the results of limit load parameter listed in Tables1, 2 and 3 (see Figure 5), it is very apparent that the accuracy of limit load parameter for regular nodal layout is higher than that of irregular layout. However, the reason of difference between two nodal layouts is not analysed here, and it will be further studied in the following research works.

CONCLUSIONS AND DISCUSSIONS

In this paper, a new formulation of upper bound approach based on RPIM and nonlinear programming is proposed. In the present method, the CTM integration method is used to calculate the internal dissipation, and the direct iterative algorithm is used to solve nonlinear programming for finding the optimal value of limit loading parameter of vertical slope. By the classical vertical slope stability problem, the validity of the present method is verified in this paper. The accuracy of limit loading parameter mainly depends on the number of field nodes and integral points. On the other hand, the accuracy of limit loading parameter for regular nodal layout is higher than that of irregular layout. The reasons of different accuracy need to be further studied. It may be carried out from the following two aspects, i.e., the CTM integration method and interpolation of RPIM shape function.

ACKNOWLEDGMENTS

The first author appreciates the useful comments from Prof H.S. Yu of University of Nottingham. The work was partly supported by Research Grants Council of Hong Kong (under grant No. 623609).

REFERENCES

Anderheggen, E., Knöpfel, H. (1972). "Finite element limit analysis using linear programming", *International Journal of Solids and Structures*, 8, 1413-1431.

Beissel, S., Belytschko T. (1996). "Nodal integration of the element-free Galerkin method", *Computer Methods in Applied Mechanics and Engineering*, 139, 49-74.

Belytschko, T., Lu, Y.Y., Gu, L. (1994). "Element-free Galerkin methods", *International Journal for Numerical Methods in Engineering*, 37, 229-256.

Bottero, A., Negre, R., Pastor, J., Turgeman, S. (1980). "Finite Element Method and Limit Analysis Theory for Soil Mechanics Problems", *Computer Methods in Applied Mechanics and Engineering*, 22, 131-149.

Capsoni, A., Corradi, L. (1997). " A finite element formulation of the rigid plastic limit analysis problem", *International Journal for Numerical Methods in Engineering*, 40, 2063-2086.

Chen, J.S., Wu, C.T., Yoon, S., You, Y. (2001). "A stabilized conforming nodal integration for Galerkin mesh-free methods", *International Journal for Numerical Methods in Engineering*, 50, 435-466.

Chen, J.S, Yoon, S., Wu, C.T. (2002). "Non-linear version of stabilized conforming nodal integration for Galerkin mesh-free methods", *International Journal for Numerical Methods in Engineering*, 53, 2587-2615.

Chen, W.F. (1975). "Limit Analysis and Soil Plasticity", New York: Elsevier Scientific Publishing Co.

Chen, S., Liu, Y., Cen, Z. (2008). "Lower-bound limit analysis by using the EFG method and non-linear programming", *International Journal for Numerical Methods in Engineering*, 74, 391-415.

Chen, Z. (2002). "Limit analysis of the classic problems of soil mechanics", *Chinese Journal of Geotechnical Engineering*, 24(1), 1-11. (in Chinese)

Ciria, H., Peraire, J., Bonet, J. (2008). "Mesh adaptive computation of upper and lower bounds in limit analysis", *International Journal for Numerical Methods in Engineering*, 75, 899-944.

Drucker, D.C., Prager, W. (1952). "Soil mechanics and plastic analysis or limit design", *Quarterly of Applied Mathematics*, 10(2), 157-165

Kim, J., Salgado, R., Yu, H.S. (1999). "Limit analysis of soil slopes subjected to pore-water pressures", *Journal of Geotechnical and Geoenvironmental Engineering*, ASCE, 125(1), 49-58.

Kim, J., Salgado, R., Lee, J. (2002). "Stability analysis of complex soil slopes using limit analysis", *Journal of Geotechnical and Geoenvironmental Engineering*, ASCE, 128(7), 546-557.

Khosravifard, A., Hematiyan, M.R. (2010). “A new method for meshless integration in 2D and 3D Galerkin meshfree methods”, *Engineering Analysis with Boundary Elements*, 34, 30-40.
Krabbenhøft, K., Lyamin, A.V., Sloan, S.W. (2007). “Formulation and solution of some plasticity problems as conic programs”, *International Journal of Solids and Structures*, 44, 1533-1549.
Krabbenhøft, K., Lyamin, A.V., Sloan, S.W. (2008). “Three-dimensional Mohr-Coulomb limit analysis using semidefinite programming”, *Communications in Numerical Methods in Engineering*, 24, 1107-1119.
Le, C.V., Gilbert, M., Askes, H. (2009). “Limit analysis of plates using the EFG method and second-order cone programming”, *International Journal for Numerical Methods in Engineering*, 78, 1532-1552.
Le, C.V., Nguye-Xuan, H., Nguyen-Dang, H. (2010a). “Upper and lower bound limit analysis of plates using FEM and second-order cone programming”, *Computer and Structures*, 88, 65-73.
Le, C.V., Nguye-Xuan, H., Askes, H., Bordas, S. P. A., Rabczuk, T., Nguyen-Vinh, H. (2010b). “A cell-based smoothed finite element method for kinematic limit analysis”, *International Journal for Numerical Methods in Engineering*, 83, 1651-1674.
Li, H.X., Yu, H.S. (2006). “Limit analysis of 2-D and 3-D structures based on an ellipsoid yield criterion”, *Acta Geotechnica*, 1, 179-193.
Liu, G.R. (2010). “Meshfree method: moving beyond the finite element method, 2nd ed.”, *CRC press: Boca Raton, USA*.
Liu, G.R., Gu, Y.T. (2005). “An introduction to meshfree methods and their programming”, *Spring*.
Liu, Y.H., Cen, Z.Z., Xu, B.Y. (1995). “A numerical method for plastic limit analysis of 3-D structures”, *International Journal of Solids and Structures*, 32(12), 1645-1658.
Lyamin, A.V., Sloan, S.W. (2002). “Upper bound limit analysis using linear finite elements and non-linear programming”, *International Journal for Numerical and Analytical Methods in Geomechanics*, 26, 181-216.
Lysmer, J. (1970). “Limit analysis of plane problems in soil mechanics”, *Journal of the Soil Mechanics and Foundations Division*, ASCE, 96(4), 1311-1334.
Makrodimopoulos A., Martin, C.M. (2006). “Lower bound limit analysis of cohesive-frictional materials using second-order cone programming”, *International Journal for Numerical Methods in Engineering*, 66, 604-634.
Makrodimopoulos A., Martin, C.M. (2007). “Upper bound limit analysis using simplex strain elements and second-order cone programming”, *International Journal for Numerical and Analytical Methods in Geomechanics*, 31, 835-865.
Makrodimopoulos A., Martin, C.M. (2008a). “Upper bound limit analysis using discontinuous quadratic displacement fields”, *Communications in Numerical Methods in Engineering*, 24, 911-927.
Martin, C.M., Makrodimopoulos A. (2008b). “Finite-Element Limit Analysis of Mohr-Coulomb Materials in 3D Using Semidefinite Programming”, *Journal of Engineering Mechanics*, ASCE, 134(4), 339-347.
Makrodimopoulos A. (2010). “Remarks on some properties of conic yield restrictions in limit analysis”, *International Journal for Numerical Methods in Biomedical Engineering*, 2010, 26, 1449-1461.
Pastor, J., Thai, T.H., Francescato, P. (2000). “New bounds for the height limit of a vertical slope”, *International Journal for Numerical and Analytical Methods in Geomechanics*, 24, 165-182.
Sloan, S.W. (1988). “Lower bound limit analysis using finite elements and linear programming”, *International Journal for Numerical and Analytical Methods in Geomechanics*, 12, 61-77.
Sloan, S.W. (1989). “Upper bound limit analysis using finite elements and linear programming”, *International Journal for Numerical and Analytical Methods in Geomechanics*, 13, 263-282.
Sloan, S.W., Kleeman, P.W. (1995). “Upper bound limit analysis using discontinuous velocity fields”, *Computer Methods in Applied Mechanics and Engineering*, 127, 293-314.
Wang, J.G., Liu, G.R. (2002). “A point interpolation meshless method based on radial basis functions”, *International Journal for Numerical Methods in Engineering*, 54 (11), 1623-1648.
Yu, H.S., Salgado, R., Sloan, S.W., Kim, J.M. (1998). “Limit analysis versus limit equilibrium for slope stability”, *Journal of Geotechnical and Geoenvironmental Engineering*, ASCE, 124(1), 1-11.
Zhang, P., Lu, M., Hwang, K. (1991). “A mathematical programming algorithm for limit analysis”, *ACTA MECHANICA SINICA*, 23(4), 433-442. (in Chinese)
Zouain, N., Herskovits, J., Borges, L.A., Feijóo, R.A. (1993). “An iterative algorithm for limit analysis with nonlinear yield functions”, *International Journal of Solids and Structures*, 30, 1397-1417.